On the Average Harvested Energy of Directive Lightwave Power Transfer (DLPT)

Vasilis K. Papanikolaou, *Graduate Student Member, IEEE*, Panagiotis D. Diamantoulakis, *Senior Member, IEEE*, Harilaos G. Sandalidis, Ranjan K. Mallik, *Fellow, IEEE*, and George K. Karagiannidis, *Fellow, IEEE*

***Abstract*—We investigate the impact of the channel statistics on the average harvested energy when directive lightwave power transfer (DLPT) is used for both indoor and outdoor environments. More specifically, for the indoor scenario, the channel randomness is subject to misalignment effects, while for the outdoor one, atmospheric turbulence is further considered. For both scenarios, closed-form expressions are extracted for the average harvested power, validated via Monte Carlo simulations. Interestingly, the final expressions help to assess the energy harvesting capabilities of a DLPT system and provide valuable insights for hardware implementation.**

***Index Terms*—Energy harvesting, free space optics, lightwave power transfer, wireless power transfer.**

I. Introduction

WIRELESS power transfer (WPT) via electromagnetic radiation has been recognized as a promising direction to improve energy sustainability in the design of the next-generation wireless networks, characterized by the rapidly increasing number of mobile devices and Internet-of-Things (IoT) sensors [1]. To this direction, lightwave power transfer (LPT) started being under consideration after seminal works, such as [2], where the effectiveness of this technique utilizing artificial light sources was proposed, for both indoors and outdoors. LPT can be implemented through several different architectures, but most commonly with an LED transmitter, a laser, or even an array of optical sources usually pointing to a solar cell [3]. Similarly to radio-frequency (RF) enabled WPT, depending on the transmitter radiation pattern, LPT systems can be directive or non-directive. Directive LPT (DLPT) can supply enough energy for IoT operations, cell phone charging, and even to power lightweight BSs, contributing to the ease of installation.

A DLPT technique was described in [2], where the authors demonstrated that several watts of power can be transferred during darkness hours to drive outdoor small cell BSs (SCBSs) using a laser-array-based transmitter. Another example of DLPT systems is the laser power beaming technique [4], which has the potential to provide high amounts of power over large distances and attracted particular interest even for space applications [5]. In this respect, distributed laser charging (DLC) has been proposed in [6], focusing on charging mobile devices indoors in a safe manner by stopping the laser beam propagation when the line of sight is blocked. In [7], simultaneous lightwave information and power transfer (SLIPT) was introduced, highlighting its differences compared to the RF-based counterpart. Furthermore, an outdoor application of SLIPT was showcased in [8], where SLIPT was utilized to power an aerial base station while also enabling its front-hauling. Likewise, in the seminal work of [9], the synergy of free space optics (FSO) and RF in delivering energy and information was investigated, with the main focus being on the optimization of the outage probability and throughput subject to an energy consumption constraint. More recently, in [10], the authors quantified the trade-off between the harvested power and the achievable data rate in a SLIPT system by optimizing the DC operating point. Interestingly, due to the solar cell response, the harvested power in LPT systems was proven in [2], [7] to be a non-linear function of the received power, complicating the mathematical tractability [11], especially when the stochastic nature of the DLPT channel is considered. Also, depending on indoor or outdoor environments, the DLPT channel statistics can vary. More specifically, in the free-space outdoor scenario, the atmospheric turbulence can deteriorate the signal, while indoor DLPT experiences mostly misalignment errors.

To address the aforementioned issues, in this work, we investigate the impact of the channel statistics on the average harvested power of DLPT, considering the non-linear output of the EH circuit. Note that similar works exist for the RF-based WPT, e.g., [12], but due to the complicated form of the harvested power from solar cells, there is a lack of similar works

Manuscript received March 24, 2021; accepted April 7, 2021. Date of publication April 13, 2021; date of current version July 9, 2021. This work was supported by COST Action CA19111 (European Network on Future Generation Optical Wireless Communication Technologies, NEWFOCUS), through COST (European Cooperation in Science and Technology). The work of Vasilis K. Papanikolaou, Panagiotis D. Diamantoulakis, and George K. Karagiannidis was supported by Greece and the European Union (European Social Fund-ESF) through the Operational Programme "Human Resources Development, Education, and Lifelong Learning 2014–2020" in the context of the project "Energy Autonomous Mobile Communication Systems With Wireless Power Transfer" under Grant 5047877. The work of Ranjan K. Mallik was supported in part by the Science and Engineering Research Board, a Statutory Body of the Department of Science and Technology, Government of India, under the J. C. Bose Fellowship. The associate editor coordinating the review of this article and approving it for publication was H. T. Dinh. *(Corresponding author: Ranjan K. Mallik.)*

Vasilis K. Papanikolaou, Panagiotis D. Diamantoulakis, and George K. Karagiannidis are with the Department of Electrical and Computer Engineering, Aristotle University of Thessaloniki, 54 124 Thessaloniki, Greece (e-mail: vpapanikk@auth.gr; padiaman@auth.gr; geokarag@auth.gr).

Harilaos G. Sandalidis is with the Department of Computer Science and Biomedical Informatics, University of Thessaly, 35 131 Lamia, Greece (e-mail: sandalidis@dib.uth.gr).

Ranjan K. Mallik is with the Department of Electrical Engineering, Indian Institute of Technology Delhi, New Delhi 110016, India (e-mail: rkmallik@ee.iitd.ernet.in).

Digital Object Identifier 10.1109/LWC.2021.3072946

for DLPT. In more detail, we derive closed-form expressions for the average of the harvested power assuming two distinctive scenarios, i.e., an indoor and a long-range outdoor one, while the mathematical derivations are validated via Monte Carlo simulations. It is further noted that the results could be utilized as a practical design guide for such systems.

II. Energy Harvesting Model

We assume that a laser or LED transmitter is used to wirelessly transfer energy to a solar-cell based energy harvesting receiver (EHR), via a directive optical link of wavelength λ and a beamwidth angle of θ_T. We further assume a Gaussian spatial intensity profile of beam waist $w_{\rm z}$ on the receiver at distance z from the transmitter and a circular EHR aperture of radius *r*.

The output current of the EHR can be expressed through the electrical equivalent of the solar cell given by [8], [13]

$$I = I_L - I_0\left(\exp\left(\frac{(V+IR_s)}{nV_{\rm T}}\right)-1\right) - \frac{V+IR_{\rm S}}{R_{\rm SH}}, \quad (1)$$

where $V_{\rm T}$ is the thermal voltage and I_0 is the dark saturation current of the solar cell, *V* is the voltage across the output terminal, $R_{\rm S}$ is the series resistance, *n* is the diode ideality factor, $R_{\rm SH}$ is the shut resistance, and $I_{\rm L}$ is the photogenerated current given by

$$I_L = \eta P_{\rm opt,r}, \quad (2)$$

with η being the responsivity of the EHR and $P_{\rm opt,r}$ the received optical power at the EHR.

Taking (1) into account and the expression $P = IV$, the harvested power can be calculated through an *I-V* sweep. Let $I_{\rm MP}$ and $V_{\rm MP}$ denote the current and voltage value, respectively, at the maximum power point in the I-V sweep. At this point, the entire photovoltaic system operates with maximum efficiency and produces its maximum output power. Thus, the maximum harvested power is expressed as $P_{\rm H} = I_{\rm MP}\,V_{\rm MP}$, which can be expressed via the fill factor, *F*, and the corner point of the *I-V* curve, ($I_{\rm sc}$, $V_{\rm oc}$), with $I_{\rm sc}$ and $V_{\rm oc}$ being the short-circuit current and the open-circuit voltage, respectively. It is noted that *F* can be seen as a quality measure of the solar cell, in the sense that higher values of *F* lead to a more square-like *I-V* sweep. Moreover, the fill factor is given by [8], [13]

$$F = \frac{P_{\rm H}}{P_{\rm T}} = \frac{I_{\rm MP}\,V_{\rm MP}}{I_{\rm sc}\,V_{\rm oc}}, \quad (3)$$

where $P_{\rm T} = I_{\rm sc}\,V_{\rm oc}$ is the theoretical power that would be the output at both the open-circuit voltage and short-circuit current together. Note that typical values of the fill factor range from 0.5 to 0.82. Thus, by using the Maximum Power Point Tracking (MPPT) method operating at the maximum power point in the I-V sweep, $P_{\rm H}$ is given by [14]

$$P_{\rm H} = FI_{\rm sc}\,V_{\rm oc}. \quad (4)$$

In order to properly utilize the LPT system, the adoption of high quality solar cells is assumed, which is translated to low values of I_0, and $R_{\rm S}$ and a high $R_{\rm SH}$. Following this practical hypothesis and by using (1), the short-circuit current is expressed as $I_{\rm sc} = I_{\rm L}$, and the open-circuit voltage as

$$V_{\rm oc} = nV_T\log\left(1+\frac{I_{\rm L}}{I_0}\right). \quad (5)$$

Finally, due to the high directivity, the system is prone to misalignment errors. On top of that, fluctuations in signal intensity due to atmospheric turbulence can also occur in outdoor systems. The combined effect at the receiver can be modeled as

$$P_{\rm opt,r} = hP_{\rm opt}, \quad (6)$$

where $P_{\rm opt}$ is the transmitted optical power, as it is transmitted from a directive optical source, and *h* is the positive real-valued channel coefficient from the laser to the EHR. Considering the above, the harvested energy by the EHR is [14]

$$P_{\rm H} = F\eta hP_{\rm opt}nV_T\log\left(1+\frac{\eta hP_{\rm opt}}{I_0}\right). \quad (7)$$

III. Average Harvested Power

In order to have an estimate of the harvested energy at the receiver, we calculate the first moment of the harvested power for the two DLPT scenarios. The corresponding channel gains that are examined are presented in their respective subsections.

According to (7) and by averaging over the random channel realization, the average harvested power over the channel gain is expressed as

$$\begin{aligned}\mathbb{E}_h[P_{\rm H}] &= \int_0^\infty F\eta hP_{\rm opt}V_T\log\left(1+\frac{\eta hP_{\rm opt}}{I_0}\right)f_h(h)\,dh \\ &= C\int_0^\infty h\log(1+Ah)f_h(h)\,dh, \end{aligned} \quad (8)$$

where $f_h(h)$ is the PDF of the channel gain, $C = F\eta P_{\rm opt}\,V_T$, and $A = \eta P_{\rm opt}/I_0$. Based on this, the following lemmas are derived concerning the average harvested power in various channel settings.

A. Indoor DLPT

Next, we assume an indoor scenario, which can be modeled via two factors h_l and h_p as $h = h_l h_p$ [15], where h_l and h_p are the deterministic path loss and the random attenuation due to geometric spread and pointing errors, respectively, due to the light propagation and the random pointing errors, respectively.

The fraction of the collected power due to geometric spread with radial displacement *a* from the origin of the EHR can be approximated as [15] $h_p \approx A_0\exp(-2a^2/w_{\rm z_{eq}})$, where

$$w_{\rm z_{eq}}^2 = w_{\rm z}^2\frac{\sqrt{\pi}{\rm erf}(\upsilon)}{2\upsilon\exp(-\upsilon^2)}, \quad (9)$$

with $w_z = \theta_T z$ being the beam waist at distance z with a divergence angle θ_T, $\upsilon = (\sqrt{\pi}r)/(\sqrt{2}w_{\rm z})$, $2r$ being the aperture diameter, and $A_0 = [{\rm erf}(\upsilon)]^2$. By considering identical displacement for the elevation and the horizontal displacement, the radial displacement *a* follows a Rayleigh distribution with

σ_s and no misalignment is present when $\sigma_s \to 0$. Then, the PDF of h_p is given by [15]

$$f_{h_p}(h_p) = \frac{\gamma^2}{A_0^{\gamma^2}} h_p^{\gamma^2-1},\ 0 \le h_p \le A_0, \tag{10}$$

where $\gamma = w_{z_{\rm eq}}/2\sigma_{\rm s}$ is the ratio between the equivalent beam radius at the receiver and the pointing error displacement standard deviation at the receiver.

Lemma 1: The average harvested power in a DLPT system that experiences channel degradation due to misalignment effects is given by

$$\mathbb{E}_h[P_H] = C\frac{\gamma^2}{\gamma^2+1}\Bigg(A_0\log(1+AA_0) - \frac{AA_0^2}{\gamma^2+2}\,{}_2F_1(1,\gamma^2+2;\gamma^2+3,-AA_0)\Bigg) \tag{11}$$

where ${}_2F_1(\cdot,\cdot;\cdot,\cdot)$ is the Gauss hypergeometric function.

Proof: The average harvested power from (8) with only pointing errors is expressed as

$$\mathbb{E}_h[P_H] = C\int_0^{A_0} h\log(1+Ah)\frac{\gamma^2}{A_0^{\gamma^2}}h^{\gamma^2-1}dh = C\frac{\gamma^2}{A_0^{\gamma^2}}\int_0^{A_0} h^{\gamma^2}\log(1+Ah)dh. \tag{12}$$

Utilizing [16, eq. (3.194.1)] for (12) we get

$$\mathbb{E}_h[P_H] = C\frac{\gamma^2}{A_0^{\gamma^2}}\frac{1}{\gamma^2}A_0^{\gamma^2+1}\log(1+AA_0)\int_0^{A_0}\frac{h^{\gamma^2+1}}{(1+Ah)}dh. \tag{13}$$

Finally, using [16, eq. (2.728.1)] to solve the integral in (13), we get (11) and the proof is completed. ∎

B. Outdoor DLPT

In the outdoors model, atmospheric turbulence further deteriorates the signal strength. The most commonly used distribution to model the scintillation effect is the Gamma-Gamma distribution, the probability density function (PDF) of which is given by [15]

$$f_{h_a}(h_a) = \frac{2(\alpha\beta)^{(\alpha+\beta)/2}}{\Gamma(\alpha)\Gamma(\beta)}h_a^{(\alpha+\beta)/2-1}K_{\alpha-\beta}\Big(2\sqrt{\alpha\beta h_a}\Big), \tag{14}$$

where Γ is the Gamma function, $K_{\alpha-\beta}(\cdot)$ is the modified Bessel function of the second kind. Moreover, assuming plane wave propagation, α and β for a point receiver and zero inner scale can be expressed through the refractive index structure parameter of the optical link C_n^2, λ, and z, according to [17], and when $a, b \to \infty$ no atmospheric turbulence is reported. In this case, the channel gain is given by $h = h_l h_a$.

Lemma 2: The average harvested power of a DLPT system when the atmospheric turbulence follows the Gamma-Gamma distribution is expressed as

$$\mathbb{E}_h[P_H] = \frac{(\alpha\beta)^{\frac{\alpha+\beta}{2}}}{\Gamma(\alpha)\Gamma(\beta)}A^{\frac{-\alpha-\beta-2}{2}}C \times G_{2,4}^{4,1}\left[\frac{\alpha\beta}{A}\middle|\begin{matrix}-\frac{\alpha+\beta}{2}-1,\frac{\alpha+\beta}{2}\\ \frac{\alpha-\beta}{2},\frac{\beta-\alpha}{2},\frac{-\alpha-\beta-2}{2},\frac{-\alpha-\beta-2}{2}\end{matrix}\right]. \tag{15}$$

Proof: In order to evaluate the average harvested power in a Gamma-Gamma channel we plug expression (14) into (8) and we make use of the Meijer-G function. The logarithm and the Bessel *K* functions can be expressed according to [18, eqs. (11) and (14)].

Then, (8) is written as

$$\mathbb{E}_h[P_H] = C\int_0^{\infty} h\log(1+Ah)\frac{2(\alpha\beta)^{\frac{\alpha+\beta}{2}}}{\Gamma(\alpha)\Gamma(\beta)}h^{\frac{\alpha+\beta}{2}-1} \times K_{\alpha-\beta}\Big(2\sqrt{\alpha\beta h}\Big)dh = \frac{(\alpha\beta)^{\frac{\alpha+\beta}{2}}}{\Gamma(\alpha)\Gamma(\beta)} \times \int_0^{\infty} h^{\frac{\alpha+\beta}{2}}G_{2,2}^{1,2}\left[Ah\middle|\begin{matrix}1,1\\1,0\end{matrix}\right]G_{0,2}^{2,0}\left[\alpha\beta h\middle|\begin{matrix}-\\ \frac{\alpha-\beta}{2},\frac{\beta-\alpha}{2}\end{matrix}\right]dh \tag{16}$$

By making use of [18, eq. (21)], (16) can finally be expressed as (15). ∎

As expected, the average harvested power in the Gamma-Gamma turbulence scenario depends on the scintillation parameters and the solar cell characteristics.

The gamma distribution has been proposed as an approximation of the gamma-gamma distribution widely used in modeling atmospheric turbulence in FSO systems [15]. The PDF of the Gamma distribution fitted to the Gamma-Gamma model is given by

$$f_{h_a}(h_a) = \frac{\theta^{-k}}{\Gamma(k)}h_a^{k-1}\exp\left(-\frac{h_a}{\theta}\right), \tag{17}$$

where θ and k are the scale and shift parameters of the Gamma distribution derived from the scintillation parameters α and β of the Gamma-Gamma distribution by matching the first two positive moments, so that

$$k = \frac{\alpha\beta}{1+\alpha+\beta} \text{ and } \theta = \frac{1}{\alpha}+\frac{1}{\beta}+\frac{1}{\alpha\beta}. \tag{18}$$

We calculate the average harvested power when the atmospheric turbulence is modeled after a gamma distributed random variable in order to determine the approximations possible use in DLPT systems.

Lemma 3: The average harvested power of a DLPT system when the atmospheric turbulence follows the Gamma distribution is given by

$$\mathbb{E}_h[P_H] = \frac{C\theta}{\Gamma(k)}G_{3,2}^{1,3}\left[A\theta\middle|\begin{matrix}-k,1,1\\1,0\end{matrix}\right]. \tag{19}$$

Proof: In order to evaluate the average harvested power, we plug (17) into (8). Once again, we use the Meijer-G representation of the $\log(1+x)$ function [18].

$$\mathbb{E}_h[P_H] = C\int_0^{\infty} h\log(1+Ah)\frac{\theta^{-k}h^{k-1}e^{-\frac{h}{\theta}}}{\Gamma(k)}dh = \frac{C\theta^{-k}}{\Gamma(\kappa)}\int_0^{\infty} h^k e^{-\frac{h}{\theta}}G_{2,2}^{1,2}\left[Ah\middle|\begin{matrix}1,1\\1,0\end{matrix}\right]dh. \tag{20}$$

Using [19, eq. (2.24.3.1)], (20) transforms into (19) and the proof is completed. ∎

Very often a free space transmission is also hindered by misalignment or pointing errors. Using the previous PDFs for turbulence and misalignment fading, the PDF of $h = h_l h_p h_a$,

when h_a follows the Gamma-Gamma distribution is given as [20]

$$f_h(h) = \frac{\alpha\beta\gamma^2}{A_0\Gamma(\alpha)\Gamma(\beta)} G_{1,3}^{3,0}\left[\frac{\alpha\beta}{A_0}h\middle|\begin{matrix}\gamma^2\\ \gamma^2-1,\alpha-1,\beta-1\end{matrix}\right]. \quad (21)$$

In this setting, the average harvested power is given by the following lemma.

Lemma 4: The average harvested power in a DLPT system that experiences Gamma-Gamma distributed atmospheric turbulence and pointing errors is given by

$$\mathbb{E}_h[P_H] = \frac{\alpha\beta\gamma^2 A^{-2} C}{A_0\Gamma(\alpha)\Gamma(\beta)} \times G_{3,5}^{5,1}\left[\frac{\alpha\beta}{A_0 A}\middle|\begin{matrix}-2,-1,\gamma^2\\ \gamma^2-1,\alpha-1,\beta-1,-2,-2\end{matrix}\right]. \quad (22)$$

Proof: We begin the proof by plugging (21) into (8) so it is expressed as follows

$$\begin{aligned}\mathbb{E}_h[P_H] &= C\int_0^\infty h\log(1+Ah)\frac{\alpha\beta\gamma^2}{A_0\Gamma(\alpha)\Gamma(\beta)} \times G_{1,3}^{3,0}\left[\frac{\alpha\beta}{A_0}h\middle|\begin{matrix}\gamma^2\\ \gamma^2-1,\alpha-1,\beta-1\end{matrix}\right]dh \\ &= \frac{\alpha\beta\gamma^2 C}{A_0\Gamma(\alpha)\Gamma(\beta)}\int_0^\infty hG_{2,2}^{1,2}\left[Ah\middle|\begin{matrix}1,1\\ 1,0\end{matrix}\right] \times G_{1,3}^{3,0}\left[\frac{\alpha\beta}{A_0}h\middle|\begin{matrix}\gamma^2\\ \gamma^2-1,\alpha-1,\beta-1\end{matrix}\right]dh. \quad (23)\end{aligned}$$

After using [18, eq. (21)], (22) is derived and the proof is completed. ■

As expected, pointing errors deteriorate the system performance even further and a more complicated expression is needed to express for the average harvested power, since it also includes the terms related to the pointing errors.

In a similar setting with the previous case, we also examine the average harvested power when the combined effect of atmospheric turbulence and pointing errors deteriorate the optical signal, but the turbulence is modeled by the gamma distribution. In this case, the combined PDF of the channel gain is given by

$$f_h(h) = \frac{\gamma^2\theta^{-\gamma^2}A_0^{-\gamma^2}}{\Gamma(k)}h^{\gamma^2-1}\Gamma\left(k-\gamma^2,\frac{h}{A_0\theta}\right), \quad (24)$$

where $\Gamma(\cdot,\cdot)$ stands for the upper incomplete Gamma function [16].

Lemma 5: The average harvested power in a DLPT system that experiences Gamma distributed atmospheric turbulence and pointing errors is given by

$$\mathbb{E}_h[P_H] = C\frac{A^{-\xi^2-1}\gamma^2\theta^{-\gamma^2}A_0^{-\gamma^2}}{\Gamma(k)} \times G_{3,4}^{4,1}\left[\frac{1}{A_0\theta A}\middle|\begin{matrix}-\gamma^2-1,-\gamma^2,1\\ 0,k-\gamma^2,-\gamma^2-1,-\gamma^2-1\end{matrix}\right]. \quad (25)$$

Proof: We begin the proof by expressing the upper incomplete Gamma function with the help of the Meijer-G function through [21, eq. (06.06.26.0005.01)]. Following that, by plugging (24) into (8) we get

$$\begin{aligned}\mathbb{E}_h[P_H] &= C\int_0^\infty h\log(1+Ah)\frac{\gamma^2\theta^{-\gamma^2}A_0^{-\gamma^2}}{\Gamma(k)} \times h^{\gamma^2-1}\Gamma\left(k-\xi^2,\frac{h}{A_0\theta}\right)dh = C\frac{\gamma^2\theta^{-\gamma^2}A_0^{-\gamma^2}}{\Gamma(k)} \\ &\times\int_0^\infty h^{\gamma^2}G_{2,2}^{1,2}\left[Ah\middle|\begin{matrix}1,1\\ 1,0\end{matrix}\right]G_{1,2}^{2,0}\left[\frac{h}{A_0\theta}\middle|\begin{matrix}1\\ 0,k-\gamma^2\end{matrix}\right]dh. \quad (26)\end{aligned}$$

After utilizing [18, eq. (21)] once more, (25) is derived and the proof is completed. ■

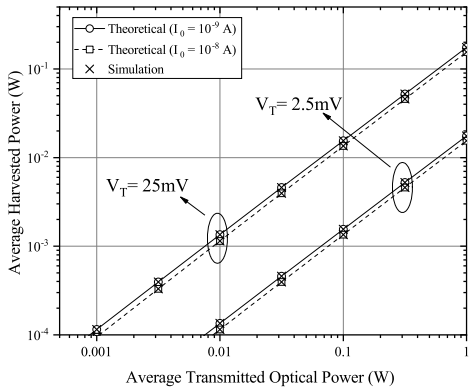

Fig. 1. Average harvested power vs Transmitted optical power for indoor scenario (z = 4m, $\sigma_s = 0.03$).

TABLE I
SIMULATION PARAMETERS [8]

z	0.5 km	λ	780 nm
ρ	0.5	σ_s	0.3
r	20 cm	θ_T	2.5 mrad
a_F (Clear)	0.43 db/km	a_F (Haze)	4.3 db/km
a_F (Rain)	5.8 db/km	a_F (Fog)	20 db/km
C_n^2 (Clear)	5×10^{-14}	C_n^2 (Haze)	1.7×10^{-14}
C_n^2 (Rain)	5×10^{-15}	C_n^2 (Fog)	5×10^{-15}
F	0.7	η	1
V_T	25 mV	I_0	10^{-9} A

TABLE II
LEAST SQUARES FITTING PARAMETERS

Indoor (I_0 [A], V_T [mV])				
	(10^{-8}, 2.5)	(10^{-9}, 2.5)	(10^{-8}, 25)	(10^{-9}, 25)
a_0	-1.754 ± 0.02	-1.72 ± 0.01	-0.754 ± 0.02	-0.72 ± 0.01
a_1	1.103 ± 0.006	1.082 ± 0.004	1.103 ± 0.006	1.082 ± 0.004
Outdoor				
	Clear	Haze	Rain	Fog
a_0	-0.74 ± 0.01	-0.096 ± 0.015	-1.04 ± 0.02	-1.754 ± 0.02
a_1	1.08 ± 0.003	1.085 ± 0.004	1.087 ± 0.005	1.103 ± 0.006
Outdoor with Misalignment				
a_0	-2.195 ± 0.03	-2.415 ± 0.03	-2.492 ± 0.03	-3.184 ± 0.05
a_1	1.113 ± 0.008	1.123 ± 0.009	1.127 ± 0.009	1.164 ± 0.015

IV. NUMERICAL RESULTS

In this section, the average harvested power is evaluated under different weather conditions both with and without the inclusion of pointing errors with regards to the transmitted optical power. Monte Carlo simulations were performed with 10^6 iterations in order to validate the theoretical analysis.

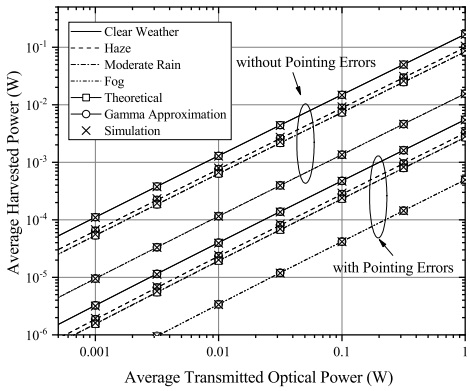

Fig. 2. Average harvested power vs Transmitted optical power for various weather scenarios.

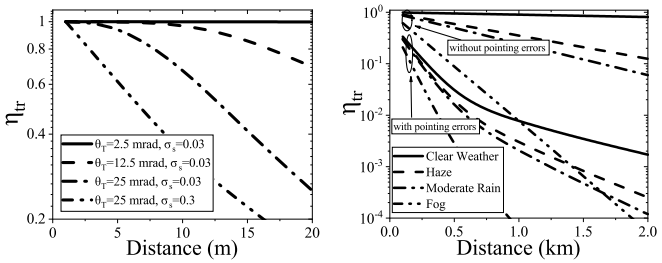

(a) Indoor (b) Outdoor

Fig. 3. Transmission Efficiency η_{Tr} for various channel conditions.

Specifically, Fig. 1 demonstrates the indoor scenario, only with pointing errors. There is a precise match between simulation and theoretical results, whereas the circuit parameters are shown to substantially affect the average harvested power. In this respect, the approximately linear relationship in the log-log plot, indicates that the average harvested power is a power function of P_{opt}, i.e., $\mathbb{E}[P_H] \approx e^{a_0} P_{\mathrm{opt}}^{a_1}$. The values of a_0 and a_1 are given in Table II, with the coefficient of determination (R squared) being around 0.99 for all curves in the examined practical range. Interestingly, a_0 is less by a value of one when V_T is lower by a factor of 10, whereas a_1 has the same value when I_0 is the same, irregardless of V_T. Despite this behavior, the increase in average harvested power, with regards to the transmitted power is lower with each increment, eventually leading to a ceiling in harvested power.

Moreover, Fig. 2 displays the average harvested power with regards to the average transmitted optical power. Clear weather conditions and fog can be considered as the upper and lower bounds of the system performance, respectively. The parameters used in the simulations can be found in Table I [8]. Note that, the gamma approximation is very close to the actual gamma-gamma results, proving to be an efficacious alternative model for turbulence description.

To express the transmission efficiency and investigate the impact of distance, the ratio of the average harvested power at distance z to the average harvested power at the at distance z_0 that corresponds to $h = 1$, which is a deterministic function of the transmitted optical power, is extracted as,

$$\eta_{\mathrm{tr}}(z) = \frac{\mathbb{E}[P_H(z)]}{\mathbb{E}[P_H(z_0)]}. \tag{27}$$

As it is shown in Fig. 3, the transmission efficiency is reduced in DLPT systems that are prone to misalignment. Also, while for the indoor DLPT a large θ_T has a detrimental effect on the transmission efficiency. Finally, as expected, outdoor DLPT systems are showing higher transmission efficiency when no pointing errors occur, while adverse weather conditions, especially fog, can substantially degrade the efficiency of the DLPT system.

REFERENCES

[1] S. Nikoletseas, Y. Yang, and A. Georgiadis, *Wireless Power Transfer Algorithms, Technologies and Applications in Ad Hoc Communication Networks*. Cham, Switzerland: Springer, 2016.

[2] J. Fakidis, S. Videv, S. Kucera, H. Claussen, and H. Haas, "Indoor optical wireless power transfer to small cells at nighttime," *J. Lightw. Technol.*, vol. 34, no. 13, pp. 3236–3258, Jul. 2016.

[3] G. Pan, P. D. Diamantoulakis, Z. Ma, Z. Ding, and G. K. Karagiannidis, "Simultaneous lightwave information and power transfer: Policies, techniques, and future directions," *IEEE Access*, vol. 7, pp. 28250–28257, 2019.

[4] K. Jin and W. Zhou, "Wireless laser power transmission: A review of recent progress," *IEEE Trans. Power Electron.*, vol. 34, no. 4, pp. 3842–3859, Apr. 2019.

[5] G. A. Landis, "Laser power beaming for lunar polar exploration," in *Proc. AIAA Propulsion Energy Forum*, Aug. 2020, pp. 1–6.

[6] Q. Liu *et al.*, "Charging unplugged: Will distributed laser charging for mobile wireless power transfer work?" *IEEE Veh. Technol. Mag.*, vol. 11, no. 4, pp. 36–45, Dec. 2016.

[7] P. D. Diamantoulakis, G. K. Karagiannidis, and Z. Ding, "Simultaneous lightwave information and power transfer (SLIPT)," *IEEE Trans. Green Commun. Netw.*, vol. 2, no. 3, pp. 764–773, Mar. 2018.

[8] P. D. Diamantoulakis, K. N. Pappi, Z. Ma, X. Lei, P. C. Sofotasios, and G. K. Karagiannidis, "Airborne radio access networks with simultaneous lightwave information and power transfer (SLIPT)," in *Proc. IEEE Global Commun. Conf. (GLOBECOM)*, Abu Dhabi, UAE, Dec. 2018, pp. 1–6.

[9] B. Makki, T. Svensson, K. Buisman, J. Perez, and M.-S. Alouini, "Wireless energy and information transmission in fso and RF-FSO links," *IEEE Wireless Commun. Lett.*, vol. 7, no. 1, pp. 90–93, Feb. 2018.

[10] S. Sepehrvand, L. N. Theagarajan, and S. Hranilovic, "Rate-power tradeoff in simultaneous lightwave information and power transfer systems," *IEEE Commun. Lett.*, vol. 25, no. 4, pp. 1249–1253, Apr. 2021.

[11] Y. Xiao, P. D. Diamantoulakis, Z. Fang, L. Hao, Z. Ma, and G. K. Karagiannidis, "Cooperative hybrid VLC/RF systems with SLIPT," *IEEE Trans. Commun.*, early access, Jan. 18, 2021, doi: 10.1109/TCOMM.2021.3051908.

[12] Y. Chen, N. Zhao, and M.-S. Alouini, "Wireless energy harvesting using signals from multiple fading channels," *IEEE Trans. Commun.*, vol. 65, no. 11, pp. 5027–5039, Nov. 2017.

[13] J. L. Gray, "The physics of the solar cell," in *Handbook of Photovoltaic Science and Engineering*, 2nd ed., Hoboken, NJ, USA: Wiley, 2011, pp. 82–129.

[14] T. Rakia, H. C. Yang, F. Gebali, and M.-S. Alouini, "Optimal design of dual-hop VLC/RF communication system with energy harvesting," *IEEE Comm. Lett.*, vol. 20, no. 10, pp. 1979–1982, Oct. 2016.

[15] M. Uysal, C. Capsoni, Z. Ghassemlooy, A. Boucouvalas, and E. Udvary, Eds., *Optical Wireless Communications*. Cham, Switzerland: Springer, 2016.

[16] I. Gradshteyn and I. Ryzhik, *Table of Integrals, Series, and Products*, 6th ed. New York, NY, USA: Academic, 2000.

[17] N. Chatzidiamantis, L. Georgiadis, H. G. Sandalidis, and G. K. Karagiannidis, "Throughput-optimal link-layer design in power constrained hybrid OW/RF systems," *IEEE J. Sel. Areas Commun.*, vol. 33, no. 9, pp. 1972–1984, Sep. 2015.

[18] V. S. Adamchik and O. I. Marichev, "The algorithm for calculating integrals of hypergeometric type functions and its realization in REDUCE system," in *Proc. Int. Symp. Symbolic Algebraic Comput.*, 1990, pp. 212–224.

[19] A. Prudnikov, Y. Brychkov, and O. Marichev, *More Special Functions* (Integrals and Series), vol. 3. New York, NY, USA: Gordon Breach Sci., 1986.

[20] H. G. Sandalidis, T. A. Tsiftsis, and G. K. Karagiannidis, "Optical wireless communications with heterodyne detection over turbulence channels with pointing errors," *J. Lightw. Technol.*, vol. 27, no. 20, pp. 4440–4445, Oct. 15, 2009.

[21] *The Wolfram Functions Site*. Accessed: Mar. 1, 2021. [Online]. Available: http://functions.wolfram.com